Mechanical Systems and Signal Processing 23 (2009) 682–689

Contents lists available at ScienceDirect

Mechanical Systems and Signal Processing

journal homepage: www.elsevier.com/locate/jnlabr/ymssp

Applications of detrended-fluctuation analysis to gearbox fault diagnosis

E.P. de Moura [a,*], A.P. Vieira [a], M.A.S. Irmão [b], A.A. Silva [c]

[a] Departamento de Engenharia Metalúrgica e de Materiais, Universidade Federal do Ceará, 60455-760 Fortaleza, CE, Brazil
[b] Colegiado de Engenharia Mecânica, Universidade Federal do Vale do São Francisco, 48909-810 Juazeiro, BA, Brazil
[c] Departamento de Engenharia Mecânica, Universidade Federal de Campina Grande, 58109-970 Campina Grande, PB, Brazil

ARTICLE INFO

Article history:
Received 9 October 2007
Received in revised form
29 April 2008
Accepted 2 June 2008
Available online 10 June 2008

PACS:
43.40.+s
43.60.+d
43.60.Cg

Keywords:
Gearbox fault diagnosis
Vibration analysis
Detrended-fluctuation analysis

ABSTRACT

Aiming at fault diagnosis, we study vibration signals obtained from gearboxes under various conditions. We consider normal gearboxes, gearboxes containing scratched gears, and gearboxes containing toothless gears, both unloaded and under load, with several rotation frequencies. By applying detrended-fluctuation analysis (DFA), a mathematical tool introduced to study fractal properties of time series, we are able to distinguish the signals with respect to their working conditions. For each signal, DFA involves performing a linear fit to the data inside intervals of a certain size, and evaluating the corresponding fluctuations detrended by the local fit. Repeating this procedure for many interval sizes yields a curve of the average fluctuation as a function of size. From the curves, we define vectors whose components correspond to the average fluctuation associated with suitably chosen interval sizes. We finally apply principal component analysis to the set of all vectors, obtaining very good clustering of the transformed vectors according to the different working conditions, with a performance comparable to that obtained from Fourier analysis, especially for gears working under load.

1. Introduction

Gearboxes are widely employed in industrial applications, lending great importance to studies aiming at gear-fault identification and characterization. The usual approach employed by those studies is to analyze vibration signals captured by an accelerometer mounted on the surface of the gear case. However, these are influenced by vibrations from many sources, such as the meshing gears, shafts, and bearings. Thus, the resulting signals are usually quite complex, hindering their analysis.

Many fault-detection techniques developed so far focus on the evolution of statistical parameters (such as standard deviation, skew, kurtosis, etc.) as a function of time [1], or on frequency analysis [2]. More recently, a series of hybrid time–frequency techniques have been developed, such as wavelet, Wigner–Ville or correlated transforms [3–9]. Both frequency and hybrid techniques rely on the identification of the frequencies present, which are then compared to models predicting which frequencies should be important in the presence of various faults.

Here we employ another approach, based on detrended-fluctuation analysis (DFA), a tool originally developed to differentiate between local patchiness and long-range correlations in DNA sequences [10]. The presence of long-range

* Corresponding author.
E-mail address: elineudo@metalmat.ufc.br (E.P. de Moura).

0888-3270/$ - see front matter © 2008 Elsevier Ltd. All rights reserved.
doi:10.1016/j.ymssp.2008.06.001

correlations (which reflects the presence of correlated noise in the sequence) is identified by studying the detrended fluctuations in the sequence, as functions of the size of the windows through which the sequence is examined. In an analogous way, one may hope that DFA can be useful in investigations of vibration signals, by filtering out noise contributions from unimportant sources, and focusing on the correlated noise which presumably comes from the gear faults. As our results show, the variation of the detrended fluctuations with the size of the time window is a signature of the type of fault present in the gear, and this signature can be captured by pattern-classification tools.

This paper is organized as follows. In Section 2 we describe the techniques employed for producing and capturing the vibration signals. Section 3 details the motivation and mathematics behind DFA. Results obtained from applying a combination of DFA and principal component analysis (PCA) to the vibration signals are presented and discussed in Section 4, and compared to results from a similar combination involving the Fourier spectra of the signals. Finally, Section 5 contains our conclusions.

2. Signal capture

All trials were performed on a especially designed bench, composed of a three-phase motor, with nominal power of 0.37 kW and nominal rotation frequency of 1555 rpm. The motor was connected to a gearbox containing four gears, but defects were only introduced to the pinion gear 1 (see Fig. 1 for the gearbox scheme). The number of teeth and the primitive diameter were 31 and 33.435 mm for gear 1, 55 and 59.319 mm for gear 2, 15 and 20.753 mm for gear 3, 57 and 73.753 mm for gear 4. The reduction factors were 1.774 between gears 2 and 1, and 3.553 between gears 4 and 3. An accelerometer was placed on the upper side of the gearbox, for signal capture, and a brake was connected to gear 4 in order to simulate a load condition. The different types of pinion gear studied were:

1. gears with no faults (normal);
2. gears with a local fault, represented by one missing tooth (toothless);
3. gears with an extensive fault, represented by a severe scratch over 10 consecutive teeth (scratched).

For each gear condition, signals were captured using six different rotation frequencies (400, 600, 800, 1000, 1200, and 1400 rpm). The motor rotation was controlled by a frequency inverter. Trials were performed both in the absence of external load or under a load of 8.4 N m, corresponding to 60% of the nominal maximum load.

For each combination of gear, frequency, and load, 18 signals were captured, resulting in a data set composed of 648 samples of vibration signals. The capture made use of a B&K4393 accelerometer coupled to a B&K2535 load amplifier. Each signal is composed of 2048 data points, with a sampling rate of 5.12 kHz, and subject to a low-pass filter with a 2 kHz cutoff.

3. Detrended-fluctuation analysis

Most techniques of time-series analysis, such as power spectra and autocorrelations, focus on identifying properties of stationary signals [11] and assume any noise present in the signals to be non-correlated. By making use of concepts introduced in the study of fractional Brownian motion (fBm) [12], one can also study memory effects in the fluctuations of a time series, in order to identify the presence of correlated noise. In a genuine fBm these memory effects are embodied by a single number, the Hurst exponent H, which governs the time evolution of the standard deviation σ associated with the

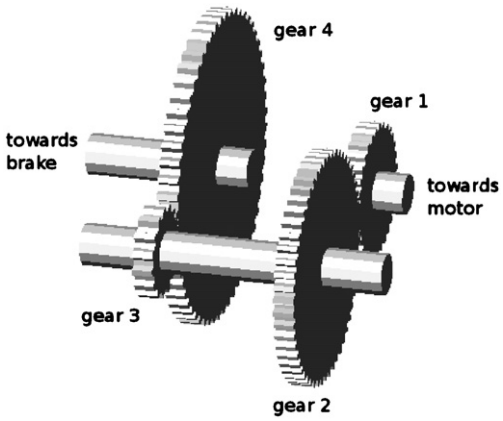

Fig. 1. Gearbox scheme, showing the four gears. Defects were introduced to gear 1.

motion. Explicitly, one has

$$\sigma = (2K_f t)^H, \tag{1}$$

where t is the time elapsed since the motion started, and K_f is a fractal diffusion coefficient. A Hurst coefficient equal to $\frac{1}{2}$ corresponds to a regular Brownian motion (i.e. Fickian diffusion), and to the absence of memory effects. Values of H different from $\frac{1}{2}$ indicate the presence of long-range memory mechanisms affecting the motion; $H > \frac{1}{2}$ ($H < \frac{1}{2}$) corresponds to persistent (antipersistent) behavior of the time series.

The DFA [10] can be used as a means of estimating the Hurst exponent of a time series by eliminating trends which could be superposed to an underlying fBm. The method consists initially in obtaining from the original series z_i (containing L points) a new integrated series $\tilde{z}_i$,

$$\tilde{z}_i = \sum_{k=1}^{i} (z_k - \langle z \rangle), \tag{2}$$

the average $\langle z \rangle$ being taken over all points,

$$\langle z \rangle = \frac{1}{L} \sum_{i=1}^{L} z_i. \tag{3}$$

After dividing the series into intervals containing τ points, the points inside a given interval are fitted by a straight line. Then, a detrended variation function Δ_i is obtained by subtracting from the integrated data the local trend as given by the fit. Explicitly, one defines

$$\Delta_i = \tilde{z}_i - h_i, \tag{4}$$

where h_i is the value associated with point i according to the linear fit. Finally, one calculates the root-mean-square fluctuation $F_k(\tau)$ inside interval I_k as

$$F_k(\tau) = \sqrt{\frac{1}{\tau} \sum_{i \in I_k} \Delta_i^2}, \tag{5}$$

and average over all intervals. Usually, the average $F(\tau)$ behaves as

$$F(\tau) \sim \tau^{\alpha} \tag{6}$$

at least inside some range of values of τ, and the scaling exponent α provides an estimate of the Hurst exponent of the underlying fBm.

On the other hand, from a signal-processing point of view, DFA can be seen as a transformation yielding the function $F(\tau)$, which compresses the information content of the time series into a much smaller number of variables. (In the case of the vibration signals considered here, each original series contains 2048 points, whereas the corresponding $F(\tau)$ curves were calculated for a maximum of 37 values of τ.) The curves $F(\tau)$ representing the various working conditions can then be used in conjunction with statistical tools aiming at pattern classification.

4. Results and discussion

Fig. 2 shows representative signals obtained from the three types of gear, working under load at a rotation frequency of 1400 rpm. Also shown are the corresponding DFA curves. The DFA was performed by selecting a fixed set $\{\tau_j\}$ of d values of the window size τ and calculating for each signal i the values $F(\tau_j)$. These values can be interpreted as the components of a vector $\mathbf{x}_i$,

$$\mathbf{x}_i = \begin{pmatrix} F(\tau_1) \\ F(\tau_2) \\ \vdots \\ F(\tau_d) \end{pmatrix}_i. \tag{7}$$

The window sizes we used for the vectors correspond to $\{4, 5, 6, 7, 8, 10, 11, 13, 16, 19, 23, 27, 32\}$, so that each vector has $d = 13$ components (other choices of the window sizes lead to similar results). We then grouped the resulting vectors according to the rotation frequency and to the presence or absence of load, and applied (PCA) [13] to each group.

Given a set of (column) vectors $\{\mathbf{x}_i\}$, containing N vectors, PCA works by projecting the vectors onto the directions defined by the eigenvectors of the group-covariance matrix $\mathbf{S}$, defined as

$$\mathbf{S} = \frac{1}{N} \sum_{i=1}^{N} (\mathbf{x}_i - \mathbf{m})(\mathbf{x}_i - \mathbf{m})^{\mathrm{T}} \tag{8}$$

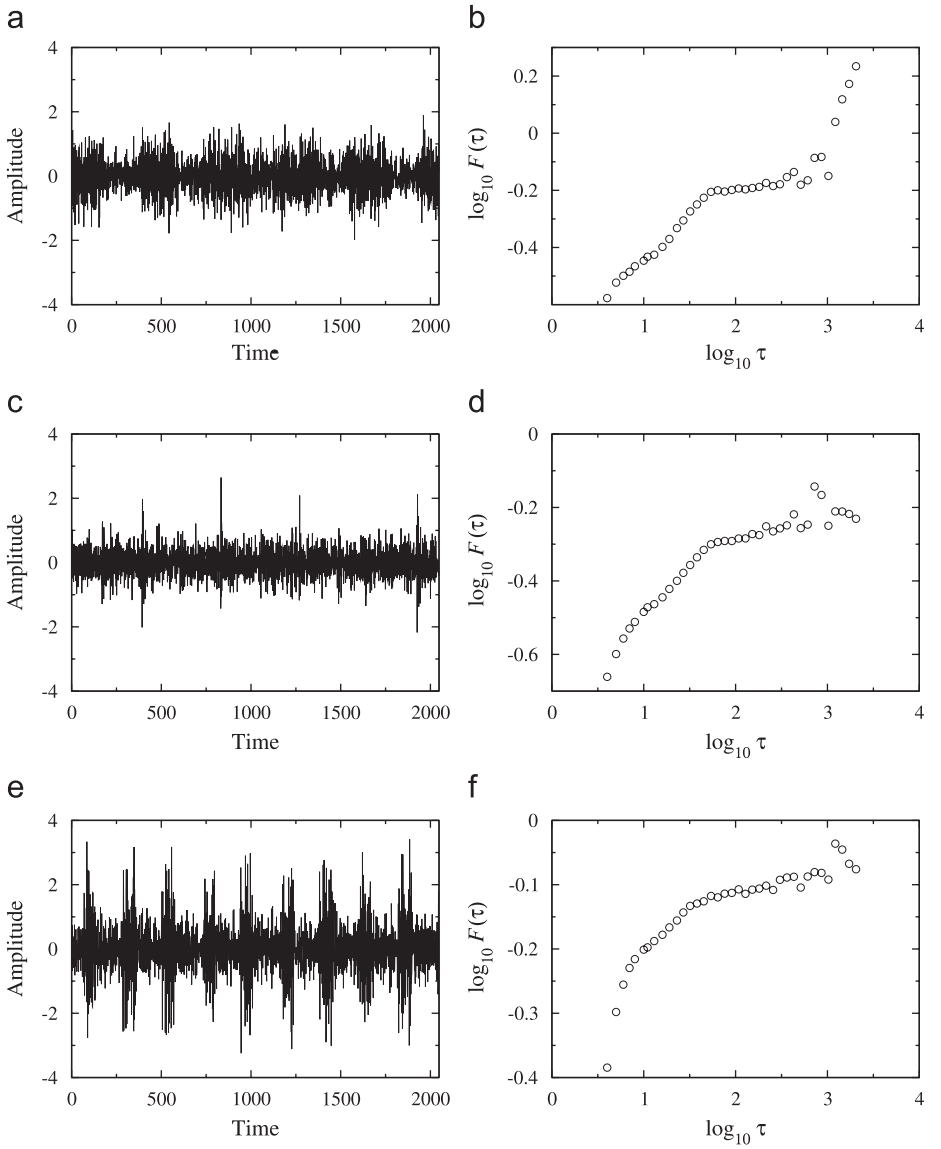

Fig. 2. Representative signals and DFA curves obtained from the three types of gear, working under load at a rotation frequency of 1400 rpm. In the signal plots, time is measured in units of the inverse sampling rate: (a) signal from normal gear, (b) DFA from normal gear, (c) signal from toothless gear, (d) DFA from toothless gear, (e) signal from scratched gear, and (f) DFA from scratched gear.

in which **m** is the average vector,

$$\mathbf{m} = \frac{1}{N}\sum_{i=1}^{N}\mathbf{x}_i \tag{9}$$

and T denotes the vector transpose. The projection along the direction of the eigenvector corresponding to the largest eigenvalue of **S** is the first principal component, and accounts for the largest amount of variation in the original vectors. The remaining principal components are arranged in decreasing order of the corresponding eigenvalues. Since it looks for the combination of window sizes yielding the largest variations among all DFA vectors, PCA is in principle able to identify the distinctive features introduced by each type of fault. For instance, our results indicate that the first principal component has comparable projections along most of the window sizes, suggesting that the average slope of a DFA curve is an important classification feature.

Figs. 3 and 4 show plots of the second versus the first principal components calculated from the DFA results obtained for all studied rotation frequencies, both in the absence and in the presence of external load. For the unloaded signals (Fig. 3), all frequencies allow for a clear discrimination of the signals obtained from scratched gears, while the points corresponding to normal and toothless gears are hardly distinguishable from just the first two components. On the other hand, under load (Fig. 4) a much clearer distinction is established between the three classes of gear, especially for higher frequencies.

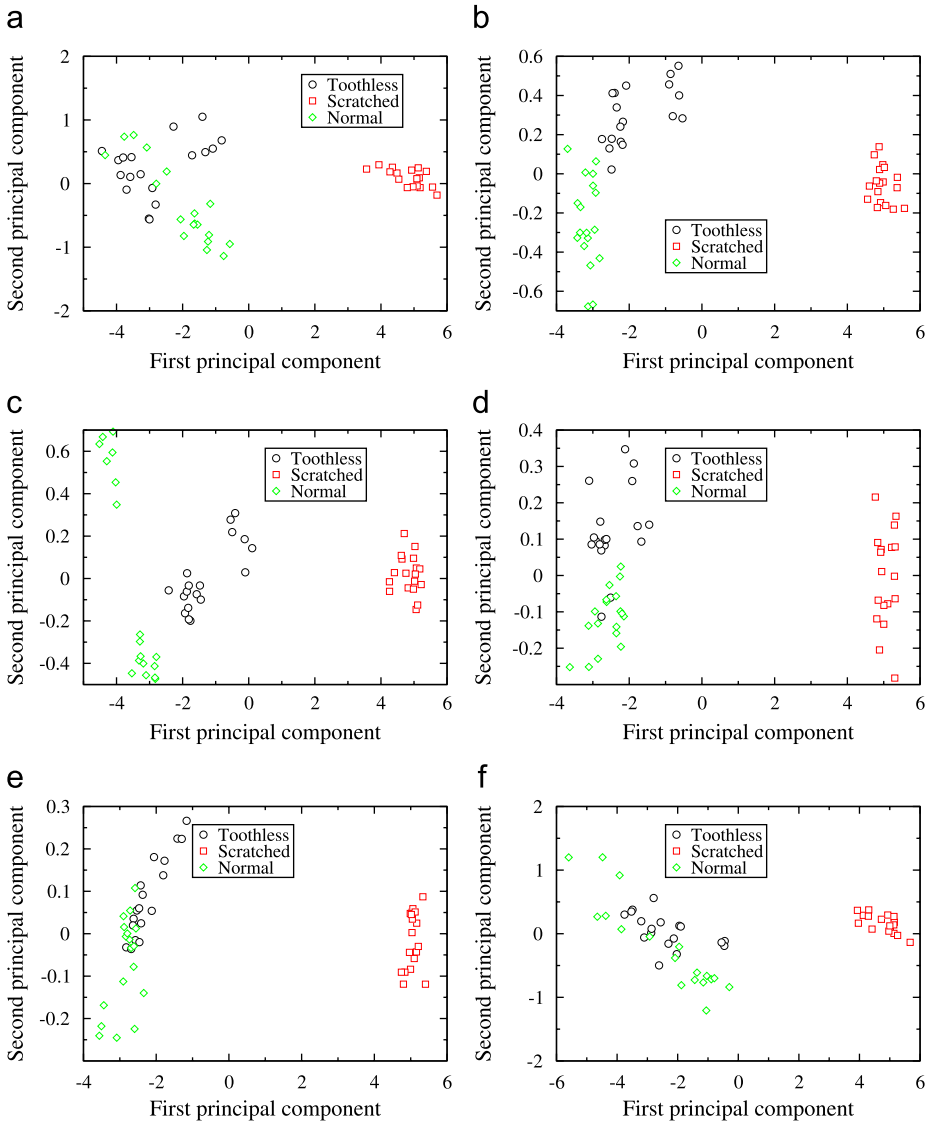

Fig. 3. Projection of the vectors corresponding to the DFA curves of signals from unloaded gears along the plane defined by the first two principal components: (a) 400 rpm, (b) 600 rpm, (c) 800 rpm, (d) 1000 rpm, (e) 1200 rpm, and (f) 1400 rpm.

In order to make a quantitative assessment of the quality of the discrimination obtained from the DFA approach, we divided the transformed vectors into a training set and a testing set, for a given group of frequency and load conditions. The training set was used to determine the average transformed vector of each class, as well as the covariance matrix, from which we built transformed vectors $\mathbf{y}_i$ containing the projections of the corresponding DFA vector $\mathbf{x}_i$ along the first three principal components, for both training and test vectors. The classification was performed by the nearest-class-mean rule, according to which each vector $\mathbf{y}_i$ is assigned to the class whose average vector lies closer to $\mathbf{y}_i$. By comparing the classification assigned by the nearest-class-mean rule with the known classification, we can evaluate the quality of the classification scheme by calculating the average percentages of gears of a given type which are correctly classified.

In the classification scheme, 36 vectors were used for training and the remaining 18 vectors for testing, and averages were taken over 100 random choices of training and testing sets. As already expected from the PCA plots (Figs. 3 and 4) all scratched gears are correctly classified, and no normal or toothless gears are misclassified as scratched. Classification errors then correspond to toothless gears classified as normal, and vice versa. Tables 1 and 2 show, for various frequencies and load conditions, the average percentage of toothless and normal gears which are correctly classified during the testing phase. These two classes are hard to distinguish, especially in the absence of load. In this case, classification errors for those two classes are around 30% or less, except at 1000 and 1400 rpm, when approximately one half of normal and toothless signals are misclassified. On the other hand, for gears working under load (Table 2), both scratched and toothless gears are

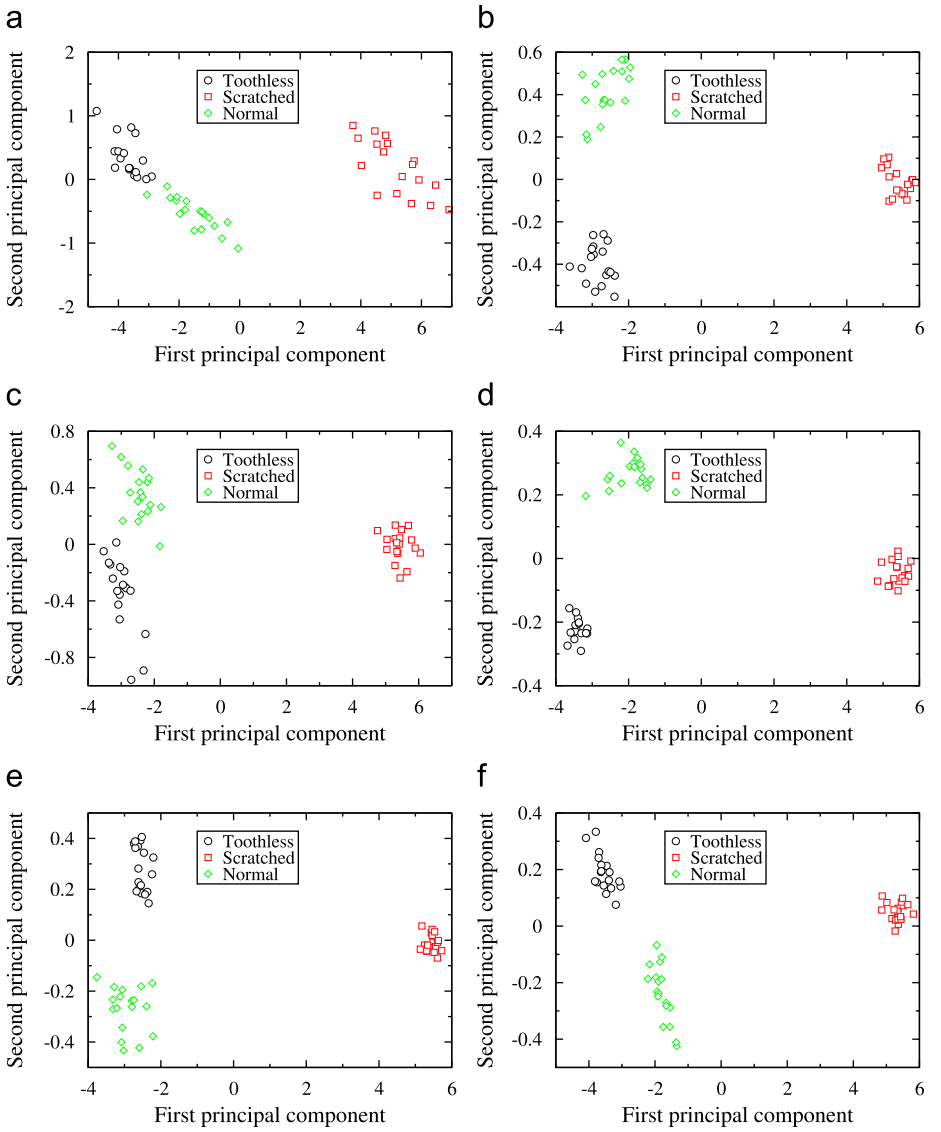

Fig. 4. Projection of the vectors corresponding to the DFA curves of signals from loaded gears along the plane defined by the first two principal components: (a) 400 rpm, (b) 600 rpm, (c) 800 rpm, (d) 1000 rpm, (e) 1200 rpm, and (f) 1400 rpm.

Table 1
Average percentage of testing signals coming from toothless and normal gears, working in the absence of load, which are correctly classified by applying the nearest-class-mean rule to the corresponding PCA-projected DFA vectors

	400 rpm	600 rpm	800 rpm	1000 rpm	1200 rpm	1400 rpm
Toothless	69.38	86.33	96.16	49.24	68.83	48.20
Normal	69.34	100	100	64.08	91.53	45.14

Table 2
The same as in Table 1, but now for gears working under load

	400 rpm	600 rpm	800 rpm	1000 rpm	1200 rpm	1400 rpm
Toothless	100	100	100	100	100	100
Normal	94.80	97.54	98.51	95.58	81.32	100

Table 3
Average percentage of testing signals coming from toothless and normal gears, working in the absence of load, which are correctly classified by applying the nearest-class-mean rule to the corresponding PCA-projected Fourier spectra

	400 rpm	600 rpm	800 rpm	1000 rpm	1200 rpm	1400 rpm
Toothless	74.20	100	100	100	99.80	95.54
Normal	66.39	87.65	100	100	97.32	83.04

Table 4
The same as in Table 3, but now for gears working under load

	400 rpm	600 rpm	800 rpm	1000 rpm	1200 rpm	1400 rpm
Toothless	89.39	100	100	100	100	100
Normal	99.16	100	100	100	100	100

always correctly classified; normal gears are mostly correctly classified, but are sometimes misclassified as toothless, with an error rate of less than 7%, except for 1200 rpm, when the error rate approaches 20%. For 1400 rpm all signals are correctly classified.

The performance of the DFA approach is comparable, although somewhat inferior, to that obtained by combining calculations of the power spectrum of the signals with PCA. Analogously to the DFA approach, we fixed the fast-Fourier transform (FFT) frequencies $\{\omega_j\}$, and defined for each signal a vector whose components are $P(\omega_j)$, the corresponding power spectral density associated with frequency ω_j. Since each time signal has 2048 points, each FFT vector has 1024 components. PCA plots for this combination (not shown) are qualitatively similar to those of the DFA-based approach. Again, in the absence of load, points corresponding to scratched gears are clearly distinct from those of the other two classes of gear, which can be rather indistinct. Under load, however, the three classes are more easily distinguishable, and for lower frequencies than in the DFA case. Tables 3 and 4 show the average percentage classification errors obtained by applying the nearest-class-mean rule with the first three principal components of the FFT. For signals from unloaded gears (Table 3), the performance is clearly superior to that of the DFA approach, except for 400 rpm. For signals obtained under load, and frequencies higher than 400 rpm, no misclassifications occur, while in the DFA approach the error rate was very low, although not zero. Notice, however, that in the DFA approach the information from all 2048 points in each signal was compressed in only 13 vector components, but still the discriminating power was almost fully preserved for the loaded signals. Also, the DFA approach is able to correctly classify all signals coming from toothless gears working under load, while the FFT approach gives only a 90% success rate for such signals at 400 rpm (compare Tables 2 and 4).

5. Conclusions

We applied a combination of detrended-fluctuation analysis (DFA) and principal component analysis (PCA) to discriminate between vibrational signals obtained from three classes of gears (normal, toothless, and scratched), under various conditions of frequency and load. For gears working under load, the performance of the method was only slightly inferior to that provided by a similar approach based on power-spectrum analysis, but with the advantage of employing a significantly smaller set of variables. Since DFA can be equally applied to both stationary and nonstationary signals, we believe that the DFA plus PCA approach could be quite useful to monitor the evolution of working conditions in gears, during which the nature of the signals would be clearly nonstationary. Presumably, one could then follow the time evolution of the PCA projections, from which gear condition could be inferred. Plans for such an experiment are being followed, and results will be reported in a future publication.

An evaluation of the efficiency of the present approach to incipient rather than severe faults will also be the subject of future studies. However, one can also apply the method to the classification of the "microstructure" of inhomogeneous media, through which the propagation of ultrasonic waves is simulated. By analyzing the time variation of the wave amplitude at a given point, representing the signal captured by a fixed transducer, the method can successfully differentiate between "microstructures" ranging from weakly to strongly disordered [14]. This represents evidence that a similar success rate might be expected when analyzing vibration signals from incipient faults.

Acknowledgments

This work was partially financed by the Brazilian agencies CNPq and FUNCAP.

References

[1] C.J. Li, J.D. Limmer, Model-based condition index for tracking gear wear and fatigue damage, Wear 241 (2000) 26–32.
[2] R.B. Randall, A new method of modeling gear faults, Journal of Mechanical Design 104 (1982) 259–267.
[3] W.J. Wang, P.D. McFadden, Early detection of gear failure by vibration analysis. 1. Calculation of the time–frequency distribution, Mechanical Systems and Signal Processing 7 (1993) 193–203.
[4] W.J. Wang, P.D. McFadden, Early detection of gear failure by vibration analysis. 2. Interpretation of the time–frequency distribution using image-processing techniques, Mechanical Systems and Signal Processing 7 (1993) 205–215.
[5] W.J. Wang, P.D. McFadden, Application of wavelets to gearbox vibration signals for fault detection, Journal of Sound and Vibration 192 (1996) 927–939.
[6] J. Lin, M.J. Zuo, Gearbox fault diagnosis using adaptive wavelet filter, Mechanical Systems and Signal Processing 17 (2003) 1259–1269.
[7] L.R. Padovese, Hybrid time–frequency methods for nonstationary mechanical signals, Mechanical Systems and Signal Processing 18 (2004) 1047–1064.
[8] A.A. Silva, M.A. Irmão, L.R. Padovese, Optimization of time–frequency representation in flaw analysis of geared systems, Revista Iberoamericana de Ingeniería Mecánica 10 (2006) 35–45 (in Portuguese).
[9] X. Fan, M.J. Zuo, Gearbox fault detection using Hilbert and wavelet packet transform, Mechanical Systems and Signal Processing 20 (2006) 966–982.
[10] C.K. Peng, V. Buldyrev, S. Havlin, M. Simmons, H.E. Stanley, A.L. Goldberger, Mosaic organization of DNA nucleotides, Physical Review E 49 (1994) 1685–1689.
[11] C. Chatfield, The Analysis of Time Series, fifth ed., Chapman & Hall/CRC, Boca Raton, 1996.
[12] P.S. Addison, Fractals and Chaos, IOP, London, 1997.
[13] A.R. Webb, Statistical Pattern Recognition, second ed., Wiley, West Sussex, 2002.
[14] R.S. do Nascimento, A.P. Vieira, L.L. Gonçalves, work in progress.